Available online at www.sciencedirect.com
ScienceDirect
Chinese Journal of Aeronautics 21(2008) 8-18
Chinese Journal of Aeronautics
www.elsevier.com/locate/cja

Active Aerothermoelastic Control of Hypersonic Double-wedge Lifting Surface

Laith K Abbas[a], Chen Qian[a,*], Piergiovanni Marzocca[b], Gürdal Zafer[c], Abdalla Mostafa[c]

[a]*Institute of Vibration Engineering Research, Nanjing University of Aeronautics and Astronautics, Nanjing 210016, China*

[b]*School of Engineering Mechanical and Aeronautical Engineering Dept. Clarkson University, Potsdam, NY 13699, USA*

[c]*Aerospace Structures, Faculty of Aerospace Engineering, Delft University of Technology, Delft 2629HS, The Netherlands*

Received 22 December 2006; accepted 9 October 2007

Abstract

Designing re-entry space vehicles and high-speed aircraft requires special attention to the nonlinear thermoelastic and aerodynamic instability of their structural components. The thermal effects are important since temperature environment brings dramatic influences on the static and dynamic behaviors of flight structures in supersonic/hypersonic regimes and is likely to cause instability, catastrophic failure and oscillations resulting in structural failure due to fatigue. In order to understand the dynamic behaviors of these "hot" structures, a double-wedge lifting surface with combining freeplay and cubic structural nonlinearities in both plunging and pitching degrees-of-freedom operating in supersonic/hypersonic flight speed regimes has been analyzed. A third order piston theory aerodynamic is used to estimate the applied nonlinear unsteady aerodynamic loads. Also considered is the loss of torsional stiffness that may be incurred by lifting surfaces subject to axial stresses induced by aerodynamic heating. The aerodynamic heating effects are estimated based on the adiabatic wall temperature due to high speed airstreams. As a recently emerging technology, the active aerothermoelastic control is aimed at providing solutions to a large number of problems involving the aeronautical/aerospace flight vehicle structures. To prevent such damaging phenomena from occurring, an application of linear and nonlinear active control methods on both flutter boundary and post-flutter behavior has been fulfilled. In this paper, modeling issues as well as numerical simulation have been presented and pertinent conclusions outlined. It is evidenced that a serious loss of torsional stiffness may induce the dynamic instability; however active control can be used to expand the flutter boundary and convert unstable limit cycle oscillations (LCO) into the stable LCO and/or to shift the transition between these two states toward higher flight Mach numbers.

Keywords: active control; aerothermoelastic analysis; freeplay; hypersonic speed

1 Introduction

Strong interactions can occur between high speed flow field and the aerospace structural components, such as wings and empennages, resulting in several important aeroelastic phenomena. These aeroelastic phenomena can dramatically influence the performance of the flight vehicle. Moreover, the tendency to reduce weight, increase structural flexibility and operating speed, certainly increase the likelihood of the flutter occurrence within the vehicle operational envelope[1-7]. However, aerospace systems inherently contain complex interactions of structural and aerodynamic nonlinearities[8]. These complex aeroelastic interactions may be so dangerous to worsen the performance of the flight vehicle because an aeroelastic system may exhibit a variety of responses that are typically associated with

*Corresponding author. Tel.: +86-25-84893221.
E-mail address: q.chen@nuaa.edu.cn

nonlinear regimes of response, including Limit Cycle Oscillations (LCO), flutter, and even chaotic vibrations[9]. Aerodynamic nonlinearities such as complex nonlinear flows with shock waves, vortices, flow separation in case of high angle of attack and aerodynamic heating. Structural nonlinearities can be subdivided into distributed nonlinearities and concentrated nonlinearities. Distributed nonlinearities are spread over the entire structure-formed material and geometric nonlinearity, while concentrated nonlinearities have local effects on a control mechanism or an attachment of external stores. Most of flight vehicles including generic missile, space shuttle and high-performance combat aircraft may have inherently concentrated structural nonlinearities such as freeplay, friction, hysteresis and preloads in the hinge part of their control surfaces and folded sections, etc. Concentrated structural nonlinearities may stem from a worn or loose hinge connection of control surfaces, joint slippages, and manufacturing tolerances. Concentrated structural nonlinearities are generally known to cause significant instability in the aeroelastic responses of aero-surfaces. Among all these several nonlinearities, the freeplay usually gives birth to the most critical flutter condition[10]. This nonlinearity often happens in control surface linkages or hinges when the surface will not move as soon as the magnitude of the input exceeds a certain value[11]. It is evidenced by wind-tunnel tests and numerical simulations that high-amplitude (low-frequency) and low-amplitude (high-frequency) steady-state LCOs may generate together with freeplay mechanism[12-13]. There have been a great number of airplanes that have experienced flutter-induced LCOs as a result of control surface freeplay[9], which, sorrowfully, are still not well published in the literature[14-15]. Control surface freeplay must be removed to increase the linearity of the measured data. Another example of the detrimental effects is the aerothermoelastic loads that play a key role in the design of the aero-surfaces of the supersonic/hyper- sonic aerospace vehicles and re-entry vehicles. Kinetic heating at high Mach numbers can seriously reduce structural stiffness. Depending on the temperature and initial conditions, the nonlinearities belong to hardening or softening spring type. The strength of metal is reduced by its exposure to a high-temperature for a period of time.

The interest in the development and application of active control technology has been prompted by the new but sometimes contradictory requirements imposed on the design of the new generation of the flight vehicle to increase structural flexibilities, high maneuverability, but meantime enhance the ability to operate safely in severe environmental conditions. The advances of active control technology have made it feasible to use active flutter suppression and active vibrations control systems in the last two decades[1,16]. A great deal of researches has been devoted to the aeroelastic active control and flutter suppression of flight vehicles. The state-of-the-art advances in these areas have been presented in Refs.[17-18]. Readers are also recommended to refer Refs.[19-20], where a number of recent contributions related to the active control of aircraft wings are fully discussed.

This paper presents an extended study of the work presented in Ref.[3]. A two-degree-of-freedom (2-DOF) airfoil system (typical section model) can provide many practical insights and useful information about the physical aeroelastic phenomena[21]. The nature of the LCO, which provides important information on the behavior of the aeroelastic system, can be examined by the nature of the Hopf bifurcation[22] of the associated nonlinear aerothermoelastic system[21,23-24]. In the aerothermoelastic governing equations, the various nonlinear effects will be incorporated. This paper also shows the combined nonlinear effects of plunge-pitch freeplay on a typical section model. The combined plunge-pitch freeplay can usually be observed in an advanced generic missile pin that could be folded at its settled position[10]. A multi-purpose military missile fin with folded mechanism may have two-axial nonlinearities at the folding fin axis and pitch control axis both, as shown in Fig.1. This paper has considered an equivalent typical section model with

2-DOF motion with freeplay nonlinearity in both plunge and pitch directions, as shown in Fig.2. An active control method will be put forward to enable the flight envelope to be expanded by increasing the flutter speed or to enhance the aeroelastic response by converting the unstable LCO into the stable one thereby suppressing LCO and chaotic dynamics. The unsteady aerodynamic forces on the airfoil are evaluated by using the third order piston theory aerodynamics (PTA), and the resulting aeroelastic equations are integrated numerically to give out the aeroelastic time responses of the airfoil motion and to show the dynamic instability.

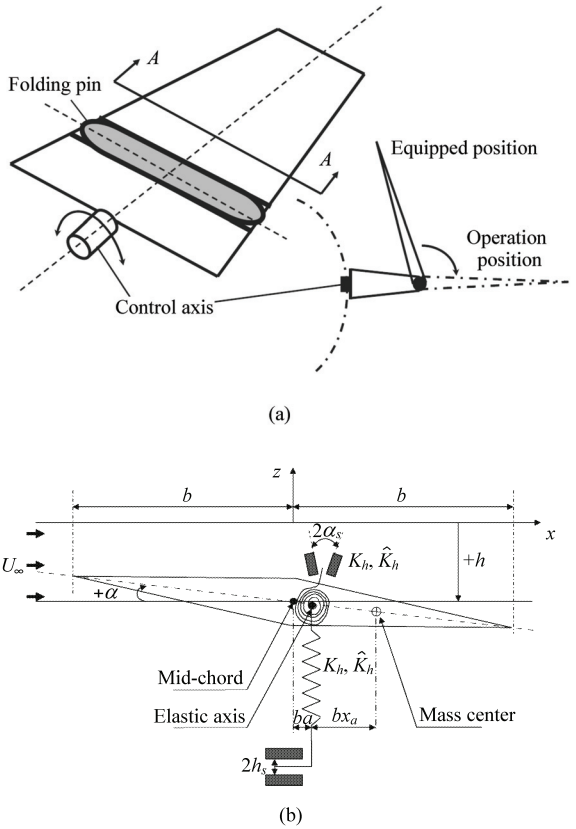

Fig.1 Typical section model.

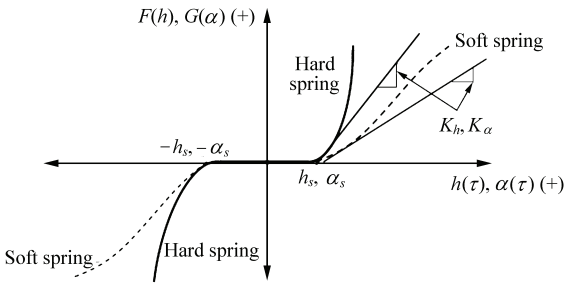

Fig.2 Freeplay nonlinear plunge and pitch stiffness.

2 Nonlinear Aerothermoelastic Control Model of 2D Lifting Surface in Supersonic/Hypersonic Speed

2.1 Nonlinear structural model

The structural model taken herein is a double-wedge 2-DOF plunging/pitching controlled airfoil. The model is free to rotate in the *x*-*z* plane and free to translate in the vertical direction as shown in Fig.1. The model accounts for nonlinear restoring force and moment from bending and torsional springs with freeplay in the 2-DOF. Consequently, the nonlinear aerothermoelastic governing equations can be written as[25]

$$m\ddot{h} + S_h\ddot{\alpha} + c_h\dot{h} + F(h) = -L(t) \tag{1}$$

$$S_\alpha\ddot{h} + I_\alpha\ddot{\alpha} + c_\alpha\dot{\alpha} + G(\alpha) = M_{\mathrm{EA}}(t) - M_C \tag{2}$$

where the plunge deflection is denoted by $h(t)$ (positive in the downward direction at the elastic axis (EA)), $\alpha(t)$ is the pitch angle about the EA (positive rotation nose up), and the superposed dots denote differentiation with respect to time t. The cubic stiffness functions (restoring force/moment) [10,21,26] (see Fig.2) can be written as follows

$$\left.\begin{aligned} F(h) &= F_a + F_b + F_c \\ G(\alpha) &= G_a + G_b + G_c \end{aligned}\right\} \tag{3}$$

$$\left.\begin{aligned} &F_a(h) = (K_h h; 0; K_h h) \\ &F_b(h_s) = (-K_h h_s; 0; K_h h_s) \\ &F_c(h) = (\hat{K}_h(h-h_s)^3; 0; \hat{K}_h(h+h_s)^3) \\ &\text{for } (h > h_s; -h_s \le h \le h_s; h < -h_s) \end{aligned}\right\} \tag{4}$$

Similar expressions for G_a, G_b and G_c can be formed by replacing the plunging variable h with the pitching variable α. Furthermore, the active nonlinear control in its simplest form can be represented in terms of the moment M_C in Eq.(2) as[3]

$$M_C = f_1\alpha(t) + f_2\alpha^3(t) \tag{5}$$

where f_1 and f_2 are the linear and nonlinear control gains, respectively.

2.2 Effective torsional stiffness

The minimum value of the effective torsional rigidity stiffness (loss in the torsional rigidity) of

instantaneously accelerated, double-wedge solid wings of constant chord and finite span subject to axial stresses induced by aerodynamic heating is[27]

$$(GJ_{\text{eff}}/GJ)_{\min}=1-0.045\,6(E\alpha_{th}/G)\times\{[T_{\text{aw}}^{(\text{f})}-T_{\text{aw}}^{(0)}]/\hat{\tau}^2\} \tag{6}$$

where GJ and GJ_{eff} are the torsional rigidity at the room temperature and the effective (apparent) torsional rigidity also on account of the additional torsional rigidity due to aerodynamic heating, respectively. In Eq.(6), E and G are the modulus of elasticity and torsional rigidity, respectively; $\hat{\tau}$ is the airfoil thickness ratio ($\equiv t_h/b$), $T_{\text{aw}}^{(0)}$ is the initial airfoil temperature at $t=0$ (initial flight Mach number $Ma_{\infty}^{(0)}$), $T_{\text{aw}}^{(\text{f})}$ is the final temperature for $t>0$ (final flight Mach number $Ma_{\infty}^{(\text{f})}$) and α_{th} is the linear coefficient of thermal expansion. In general, the adiabatic wall temperature (the concept of adiabatic wall temperature is used in the field of high velocity aerodynamics) is given by

$$T_{\text{aw}}=T_{\infty}\{1+[r(\gamma-1)Ma_{\infty}^2/2]\} \tag{7}$$

Herein γ is the isentropic gas coefficient ($\gamma=1.4$ for dry air), T_{∞} is the free stream temperature at flight altitude and r is the temperature-recovery factor and in the case of a turbulent boundary layer on a plate, $r=\sqrt[3]{Pr}$ for Prandtl numbers (Pr) close to 1. By substituting Eq.(7) into Eq.(6) with $r\approx 0.9$ and $\gamma=1.4$, the minimum torsional rigidity is

$$(GJ_{\text{eff}}/GJ)_{\min}=1-(0.008\,21)(E\alpha_{th}/G)\times T_{\infty}\{[Ma_{\infty}^{2(f)}-Ma_{\infty}^{2(0)}]/\hat{\tau}^2\} \tag{8}$$

which implies that the maximum reduction (in per cent) in torsional stiffness will depend on: (a) material $(E\alpha_{th}/G)$; (b) geometry ($\hat{\tau}$); (c) altitude (T_{∞}); and (d) velocity (Ma_{∞}^2). It is noticeable that the minimum torsional rigidity is independent on the magnitude of the heat-transfer coefficient. Taking into account the loss in the effective torsional stiffness, the torsional frequency of cantilevered beam can be written as follows

$$\omega_{\alpha}=(\pi/2L)\sqrt{[(GJ_{\text{eff}}/GJ)_{\min}GJ]/I_{\alpha}} \tag{9}$$

where L represents the beam length and I_{α} is the mass polar moment of inertia per unit length.

2.3 Nonlinear piston theory aerodynamics

The aerodynamic loads due to panel transverse motion vary rapidly and result in nearly adiabatic conditions at the edge of the boundary layer. The pressure on the upper and lower faces of the lifting surface moving with the local transverse velocity (downwash velocity) v_z may be expressed by[28-29]

$$\frac{p(x,t)}{p_{\infty}}=\{1+[\frac{(\gamma-1)}{2}](\frac{v_z}{c_{\infty}})\}^{2\gamma/(\gamma-1)} \tag{10a}$$

$$c_{\infty}^2=\gamma\,p_{\infty}/\rho_{\infty} \tag{10b}$$

where $p(x,t)$, p_{∞}, ρ_{∞} and c_{∞} are the pressure distribution as a function of time, the free stream pressure, the air density and the undisturbed speed of sound. The undisturbed speed of sound, v_z, may be expressed by

$$v_z=\pm[Z(x,t)_{,t}+U_{\infty}Z(x,t)_{,x}] \tag{10c}$$

where U_{∞} is the free stream velocity; $(*)_{,t}$, $(*)_{,x}$ are the derivative with respect to time and spatial coordinate. The sign $\pm$ denotes the upper (u) and lower (l) surfaces. In addition, the function $Z(x,t)$ represents the transversal displacement of the elastic surface from its undisturbed state[30]

$$Z(x,t)=-\{h(t)+(x-ba)\alpha(t)\}+f(x) \tag{10d}$$

where $f(x)$ represents the airfoil surface function. Assuming that values of $f_{\text{u}}(x)$ and $f_{\text{l}}(x)$ are on the upper and lower surfaces of the lifting surface, respectively. Eq.(10d) means

$$\begin{aligned}v_{z,\text{u}}&=-[\dot{h}+(x-ba)\dot{\alpha}]+U_{\infty}[-\alpha+\partial f_{\text{u}}(x)/\partial x]\\ v_{z,\text{l}}&=\ [\dot{h}+(x-ba)\dot{\alpha}]-U_{\infty}[-\alpha+\partial f_{\text{l}}(x)/\partial x]\end{aligned};$$

$$\left\langle\begin{array}{lll}\partial f_{\text{u}}(x)/\partial x=\hat{\tau} & : & -b<x<0\\ \partial f_{\text{u}}(x)/\partial x=-\hat{\tau} & : & 0<x<b\\ \partial f_{\text{l}}(x)/\partial x=-\hat{\tau} & : & -b<x<0\\ \partial f_{\text{l}}(x)/\partial x=\hat{\tau} & : & 0<x<b\end{array}\right\rangle \tag{10e}$$

where t_h is the airfoil half thickness. Eq.(10a) can be expanded into Taylor's series for variable (v_z/c_{∞}) up to the third-order inclusive gives the pressure formula for the PTA in the third-order approximation [31-32]

$$\frac{p(x,t)}{p_\infty}=1+\left[\underbrace{\gamma(\frac{v_z}{c_\infty})\eta}_{\text{Linear terms of PTA}}+\underbrace{[\gamma\frac{(\gamma+1)}{4}][(\frac{v_z}{c_\infty})\eta]^2}_{\text{Quadratic terms of PTA}}+\underbrace{[\gamma\frac{(\gamma+1)}{12}][(\frac{v_z}{c_\infty})\eta]^3}_{\text{Cubic terms of PTA}}\right] \tag{11}$$

As indicated in Ref.[32], the linear term of this expression corresponds to Ackeret's formula for the quasi-steady pressure on a thin profile in a supersonic flow field, while the quadratic term is about Busemann's formula for $Ma_\infty >> 1$. In Eq.(11), the aerodynamic correction factor $\eta = Ma_\infty / \sqrt{Ma_\infty^2 - 1}$ make it possible to extend the validity of the PTA to the entire low supersonic/hypersonic flight speed regime. Also note that Eqs.(10)-(11) are applicable as long as the transformations through compression and expansion can be seen isentropic, that is, the induced shock losses could be neglected (low intensity waves). However, Eq.(11) dose not consider the losses across a shock, nor does it accurately predict the pressure in an area associated with heavy shock interactions[31]. For more details, see Refs.[33-34]. Ref.[34] gives out a more general formula for the pressure, obtained from the theory of oblique shock waves (SWT) which is valid over the entire supersonic—hypersonic flight speed range and valid for both compression before the shock wave and expansion (assuming that the shock waves are attached to the sharp leading edge and that the flow behind these waves remains supersonic). SWT possesses a number of following advantages: (1) it takes into account for the shock losses occurring in the case of strong waves; (2) like PTA, it can be used over a larger range of angles-of-attack ($\alpha \le 20^\circ$) and Mach numbers ($Ma_\infty \ge 1.3$), and (3) it is also valid for the Newtonian speed regime ($Ma_\infty \to \infty$; $\gamma \to 1$) [34]. Ref. [32] reveals that the PTA provides more conservative results than those obtained with SWT. However, it is worth noting that the results provided by PTA, in good agreement with those out of the Euler solution, the CFL3D codes and the exact unsteady supersonic aerodynamics theory, could be applicable whenever Mach numbers exceed the hypersonic regime ($Ma_\infty > 5$) as indicated in Ref.[35].

2.4 Nonlinear aerothermoelastic governing equations

The system of governing equations in dimensionless parameters of a supersonic/hypersonic double-wedge controlled airfoil in a plunging-pitching coupled motion can be described as

$$\begin{aligned}&\xi''(\tau)+\chi_\alpha\alpha''(\tau)+2\zeta_h(\bar{\omega}/U^*)\xi'(\tau)+\\&(\bar{\omega}/U^*)^2\bar{F}_a(\xi)\xi(\tau)+(\bar{\omega}/U^*)^2\bar{F}_b(\xi_s)+\\&(\bar{\omega}/U^*)^2\bar{F}_c(\xi)[\xi^3(\tau)+3(-1)^n\xi_s\xi^2(\tau)+\\&3\xi_s^2\xi(\tau)+(-1)^n\xi_s^3]=\bar{L}(\tau)\end{aligned} \tag{12a}$$

$$\begin{aligned}&(\chi_\alpha/r_\alpha^2)\xi''(\tau)+\alpha''(\tau)+(2\zeta_\alpha/U^*)\alpha'(\tau)+\\&(1/U^{*2})\bar{G}_a(\alpha)\alpha(\tau)+(1/U^{*2})\bar{G}_b(\alpha_s)+(1/U^{*2})\bullet\\&\bar{G}_c(\alpha)[\alpha^3(\tau)+3(-1)^n\alpha_s\alpha^2(\tau)+3\alpha_s^2\alpha(\tau)+(-1)^n\alpha_s^3]=\\&\bar{M}_{EA}(\tau)-(1/U^{*2})(\varphi_1\alpha(\tau)+\varphi_2\alpha^3(\tau))\end{aligned} \tag{12b}$$

in which

$$\begin{aligned}&\bar{F}_a(\xi)=(1;0;1);\ \bar{F}_b(\xi_s)=(-\xi_s;0;\xi_s)\\&\bar{F}_c(\xi)=(\hat{\eta}_h;0;\hat{\eta}_h)\ \text{for}\ (\xi(\tau)>\xi_s, n=1;\\&-\xi_s\le\xi(\tau)\le\xi_s;\xi(\tau)<-\xi_s, n=2)\end{aligned} \tag{12c}$$

Similar expression for $\bar{G}'s$ can be acquired by replacing $\xi(\tau)$ with $\alpha(\tau)$. The primes denote differentiation with respect to dimensionless time τ. The nonlinear coefficients $\hat{\eta}_h, \hat{\eta}_\alpha$ can be positive or negative values. Positive values of $\hat{\eta}_h, \hat{\eta}_\alpha$ account for hard structural nonlinearities, while negative ones soft structural nonlinearities. α_s and ξ_s are the freeplays expressed in dimensionless form, respectively. The two normalized linear and nonlinear control gain parameters φ_1, φ_2 are defined by $\varphi_1 = f_1 / K_\alpha$ and $\varphi_2 = f_2 / K_\alpha$, respectively. Details of Eq.(12) can be found in Ref.[36].

3 Time Domain Solution in the Presence of Active Control Model

To perform the nonlinear aerothermoelastic analysis in the time domain, Eq.(12) are transformed

into a state-space matrix form

$$\dot{\boldsymbol{y}}(\tau)=\begin{bmatrix}\boldsymbol{0} & \boldsymbol{I}\\ \boldsymbol{M}^{-1}\boldsymbol{A} & \boldsymbol{M}^{-1}\boldsymbol{B}\end{bmatrix}\boldsymbol{y}(\tau)-\begin{bmatrix}\boldsymbol{0} & \boldsymbol{0}\\ \boldsymbol{0} & \boldsymbol{M}^{-1}\end{bmatrix}\boldsymbol{R}(\xi_s,\alpha_s) \tag{13a}$$

and

$$\begin{aligned}\boldsymbol{A}&=(\boldsymbol{Q}_{\mathrm{L2ext}}+\boldsymbol{Q}_{\mathrm{NL2ext}}-\boldsymbol{K}_{\mathrm{L}}-\boldsymbol{K}_{\mathrm{NL}}-\boldsymbol{M}_{\mathrm{control}})\\ \boldsymbol{B}&=(\boldsymbol{Q}_{\mathrm{L1ext}}+\boldsymbol{Q}_{\mathrm{NL1ext}}-\boldsymbol{C})\end{aligned} \tag{13b}$$

Herein the state vector and system matrices can be represented as

$$\boldsymbol{y}(\tau)=\begin{Bmatrix}\xi(\tau)\\ \alpha(\tau)\\ \dot{\xi}(\tau)\\ \dot{\alpha}(\tau)\end{Bmatrix},\ \boldsymbol{R}(\xi_s,\alpha_s)=\begin{Bmatrix}0\\ 0\\ Q_{\mathrm{f}}(1,1)\\ Q_{\mathrm{f}}(2,1)\end{Bmatrix},$$

$$\boldsymbol{M}_{\mathrm{control}}=\begin{bmatrix}0 & 0\\ 0 & (1/U^{*2})(\varphi_1+\varphi_2\alpha^2(\tau))\end{bmatrix} \tag{13c}$$

where $\boldsymbol{M}_{\mathrm{control}}$ represents the linear and nonlinear active control moment matrix. Ref.[36] gives the matrices of Eq.(13b) in detail. A numerical simulation by use of the 5-6th Runge-Kutta Fehlberg time integration scheme with step size control is carried out for the system in Eq.(13a).

4 Numerical Results and Discussions

The influences of losses in effective torsional stiffness of a solid thin double-wedge wing with various parameters such as flight condition, thickness ratio, pitch freeplay and pitching stiffness nonlinearity has been analyzed before any control is applied emphasizing the important effects of aerodynamic heating on the nonlinear aerothermoelastic behavior of the examined aerothermoelastic system. Unless otherwise stated, the numerical simulations consider the baseline parameters which are listed in Table 1.

In Fig.3, the curves show how likely this system is to lose torsional stiffness whenever aerodynamic heating is considered in conjunction with altitude and thickness ratios.

Exclusive of the aerodynamic heating, Curve #1 shows no reduction in the effective torsional stiffness at the flutter Mach number Ma_{LF}=17.40 (LF, linear flutter). It is apparent that at flight Mach number $Ma_\infty \approx 5$, Curve #2 (H = 10 000 m, $\hat{\tau}$ = 0.15, Ma_{LF} = 13.65), #3 (H = 5 000 m, $\hat{\tau}$ = 0.15, Ma_{LF} = 13.65) and #4 (H = 10 000 m, $\hat{\tau}$ = 0.05, Ma_{LF} = 4.31) have reduced torsional stiffness of the original value by 4.9%, 5.6% and 41.5%, respectively. Clearly the thickness ratio plays a detrimental role in the losses in torsional stiffness and consequently in the flutter speed and the LCO behavior of the examined aerothermoelastic lifting surface.

In Fig.4, are presented a number of bifurcation diagrams constructed from the amplitude of the pitch LCO in a function of the flight Mach number

Table 1 Baseline parameters of 2-DOF plunging-pitching airfoil

Material used Titanium (Ti-6%Al-4%V)	Parameters
Mechanical properties	ρ = 4420 kg/m^3; TEC (0-100 C°) 8.8×10^{-6}/K; TEC (0-300 C°) 9.2×10^{-6}/K; $E=114\times10^9$ N/m^2; $G=43.51\times10^9$ N/m^2; θ = 0.31
Flight condition	H =10 000 m; ρ_∞ = 0.413 5 kg/m^3; c_∞=299.53 m/s; T_∞ =223.26 K; η =1.0; γ =1.4
Airfoil geometry parameters	Section of rectangular wing; Aspect Ratio = 3.0; b = 0.50 m; $\hat{\tau}$ =0.15; m = 331.5 kg/m
Airfoil physical parameters	χ_α = 0.25; r_α = 0.5; ζ_h, ζ_α = 0; α = –0.25; $\bar{\omega}$ = 0.213 5
Cubic stiffness nonlinearities	$\hat{\eta}_h$ = 0; $\hat{\eta}_\alpha$ = 10
Initial condition	$\xi(\tau=0)=\dot{\xi}(\tau=0)=\dot{\alpha}(\tau=0)=0$; $\alpha(\tau=0)=5^\circ$
Initial freeplay	α_s=1°; ξ_s=0

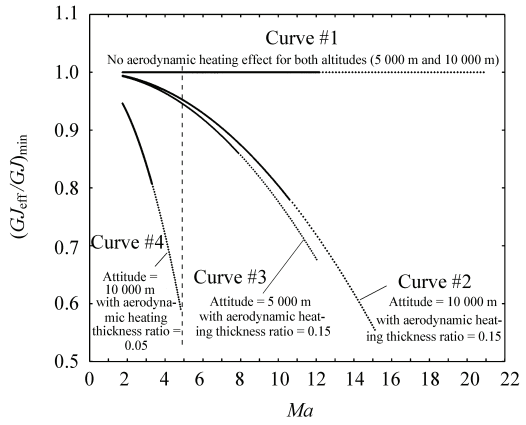

Fig.3 Reduction in torsional stiffness for solid double-wedge wing due to aerodynamic heating. Effects of thickness ratio and altitude.

for a plunging/pitching airfoil with a freeplay structural nonlinearity in pitch, cubic pitch structural nonlinearities which are subject to supersonic/hypersonic flow inducing aerodynamic heating. Because of symmetric pitch LCO amplitude and for the purpose of better graphical representation, some of the plots in Fig.4 have been presented in positive or in negative side of the LCO curve as shown later. In Fig.4(a), Case #1 (positive side of LCO curve) is of the system without aerodynamic heating at $\hat{\eta}_h = \hat{\eta}_\alpha = 0$, and $Ma_{\mathrm{LF}} = 17.40$. Case #2 (negative side), is of the system without aerodynamic heating too, but at $\hat{\eta}_h = 0$, $\hat{\eta}_\alpha = 10$ (hard structural nonlinearities) with a flutter speed the same as in Case #1. Note that in order to keep the proposed model and approach within the limits of validity, the simulations are restricted to the cases with the pitching displacement within $\pm 20°$.

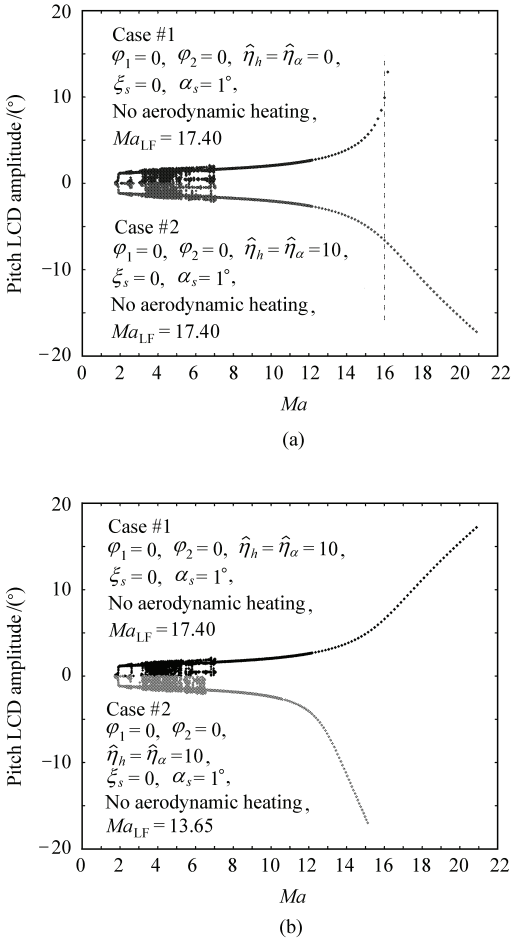

Fig.4 Bifurcation pitch diagrams for the double-wedge airfoil with nonlinearities.

The aerothermoelastic system exhibits a bifurcation behavior for Cases #1 and #2 at $Ma_\infty \approx 1.7$. In the speed range ($1.7 < Ma_\infty \le 7$), different types of response behavior (periodic, quasi-periodic or chaotic) will occur. Within the speed range ($7 < Ma_\infty \le 17$) for Case #1, ($7 < Ma_\infty \le 21$) for Case #2, a stable LCO is experienced, respectively; its amplitude increases with the increase of the flight Mach number. At $Ma_\infty \approx 16$, the Case #1 exhibits a pitch LCO with amplitude of about 9.9°, while the Case #2, the LCO has a pitching amplitude about 6.6°. It appears that cubic structural nonlinearities greatly decrease the LCO amplitude, while the linear flutter speed remains constant. Besides, Case #1 has maximum amplitude about 13° at $Ma_\infty \approx 16.2$ compared with amplitude of about 17° at $Ma_\infty \approx 21$ for Case #2. Fig.4(b) shows the effects of aerodynamic heating. Case #1 in Fig.4(b) is the same as the Case #2 in Fig.4 (a) but in positive side. The results of Case #2 reveals that the flutter speed ($Ma_{\mathrm{LF}} =$ 13.65), as well as the LCO behavior, are affected by the losses in the torsional stiffness. In both cases, the pitching structural nonlinearities are assumed to be ($\hat{\eta}_h = 0$, $\hat{\eta}_\alpha = 10$).

In Fig.5, a considerable change in the amplitude of the LCO is clearly observed in the pitch active control. In Fig.4(b), Case #1 is the same as the Case #2 but in positive side without any active control ($\varphi_1 = \varphi_2 = 0$). Case #2 ($\varphi_1 = 0.1, \varphi_2 = 10\varphi_1$), #3 ($\varphi_1 = 0.3, \varphi_2 = 10\varphi_1$), #4 ($\varphi_1 = 0.8, \varphi_2 = 10\varphi_1$), and #5 ($\varphi_1 = 1, \varphi_2 = 10\varphi_1$) present shifts of the bifurcation behavior to $Ma_\infty \approx 3.8$, 8.0, 12.5 and 13.5, respectively. The unstable LCO including the chaotic region in Case #1 has been suppressed until $Ma_\infty \approx 7$ as it is in the Case #3. Fig.5 also shows the phase portraits and time histories at various flight Mach numbers representing the uncontrolled (Case #1) and the controlled system (Cases #4 and #5), respectively. Clearly, increasing the linear pitch gain can extend the flutter boundary and convert the unstable LCO into stable LCO and/or shift the transition between these two states toward higher flight Mach numbers with suppression of LCO.

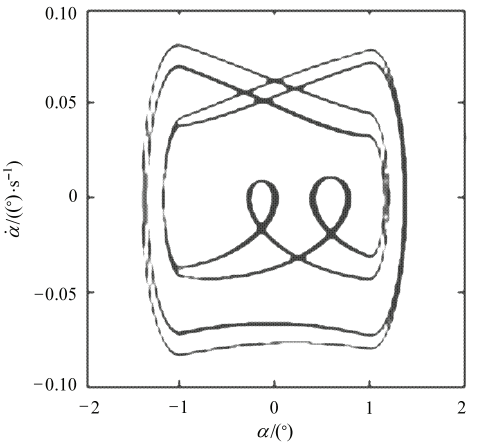

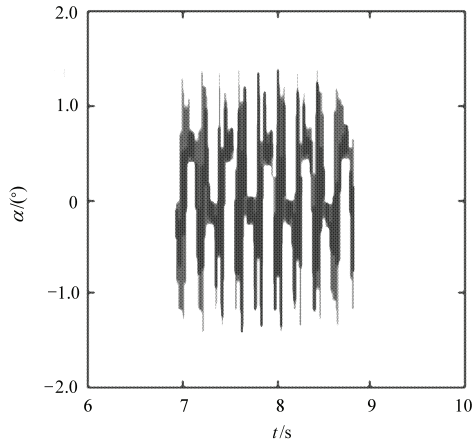

(a) Uncontrolled LCO, Ma = 2.58

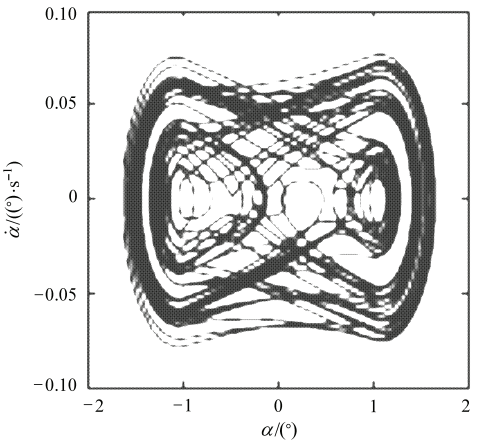

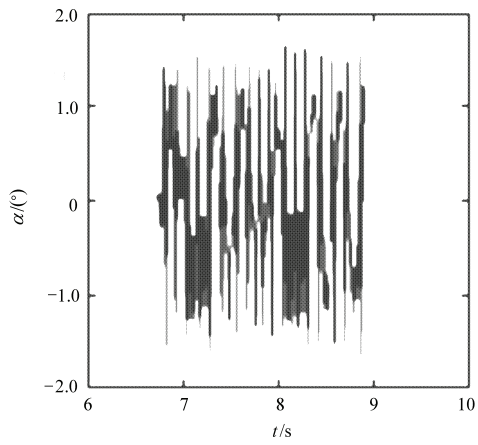

(b) Uncontrolled LCO, Ma = 4.00

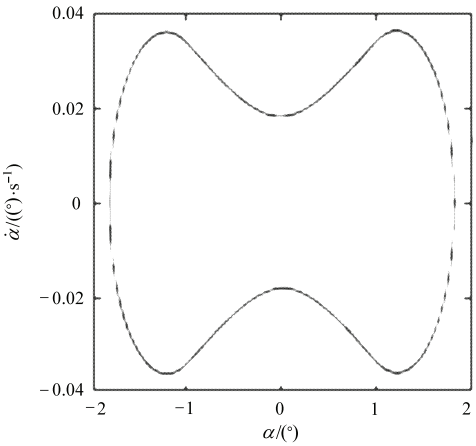

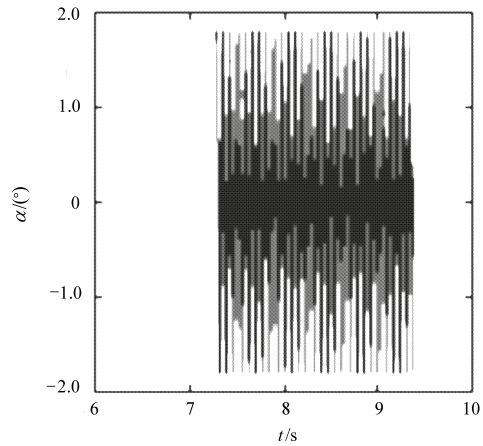

(c) Uncontrolled LCO, Ma = 8.00

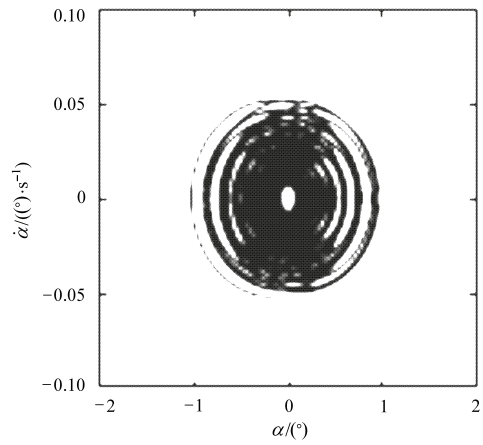

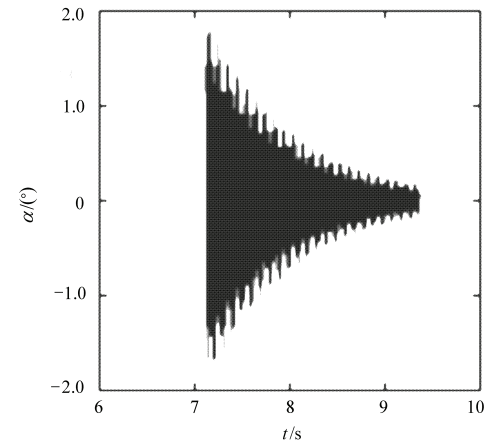

(d) Controlled LCO, Ma = 8.00 (Case #4 and Case #5)

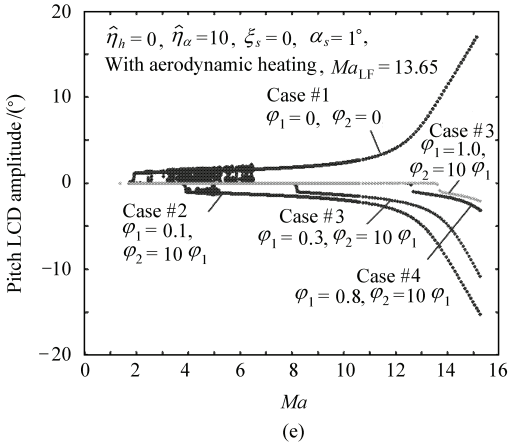

(e)

Fig.5 Pitch LCO amplitude versus flight Mach number for a 2-DOF system with all nonlinearities. Time histories and phase portraits represent the uncontrolled and controlled system, respectively.

Fig.6 shows the effects of nonlinear control gain with zero linear and non-zero nonlinear gains ($\varphi_1 = 0, \varphi_2 \neq 0$). It indicates that increasing φ_2 alone (for Case #2, $\varphi_2 = 50$ and for Case #3, $\varphi_2 = 100$) is less effective in stabilizing the aerothermoelastic system than for the linear one. This leads to a practical application of the control mechanism on actual and future generation aerospace vehicle lifting surfaces.

Unsteady aerodynamic models at very high Mach numbers might require considerations of ionization and chemical reactions. In this case modeling issues will require a more complicated approach that is most likely to obscure the important results that this paper would like to convey to reader. These issues will be discussed in subsequent works.

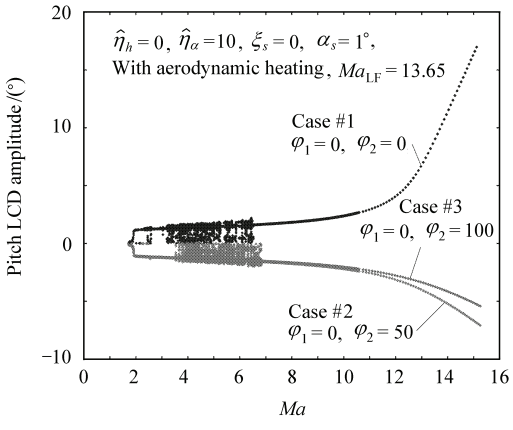

Fig.6 Effects of nonlinear active control on system encompassing all nonlinearities.

5 Conclusions

A comprehensive study is performed concerning the influences of aerodynamic heating on the nonlinear aerothermoelastic behavior of a solid thin double-wedge airfoil which is subjected to all nonlinearities (structural-freeplay and cubic stiffness, aerodynamic-third order piston theory) in supersonic/hypersonic flight speed regime. The results introduced herein will broaden the scope and enhance the reliability of the complex nonlinear aerothermoelastic analysis and design criteria of aero-surfaces. In addition, the potentiality of the linear and nonlinear active control makes it possible to extend the flutter boundary and convert the unstable aerothermoelastic behavior into the stable and/or shift the transition between these two states toward higher flight Mach numbers with suppression of LCO. Moreover, the analysis performed in this paper is able to serve as a guideline for selecting appropriate control gains to maximize the performance.

The issue of applying the active control to the hot structures is not involved. Authors believe that this problem can be solved by using a spring-like device whose linear and nonlinear characteristics can be controlled, but additional analysis is required to confirm this belief. In addition, this work constitutes the first step toward a more general investigation of the active control ability on nonlinear aerothermoelastic phenomena of a control surface moving in a supersonic/hypersonic range. To realize the more robust control strategy, this method enables researchers in the future to accomplish a study on a large number of parameters that characterize the hot structures with different active linear and nonlinear control theories such as optimal control (LQR and others).

References

[1] Marzocca P, Librescu L, Chiocchia G. Aeroelastic response of 2-D lifting surfaces to gust and arbitrary explosive loading signatures. Int J Impact Engineering 2002; 25(1): 41-65.

[2] Marzocca P, Librescu L, Silva W A. Aeroelastic response of nonlinear wing section by functional series technique. AIAA J,

2002; 40(5): 813-824.

[3] Marzocca P, Librescu L, Silva W A. Flutter, post-flutter and control of a supersonic 2-D lifting surface. J Guidance, Control, and Dynamics 2002; 25(5): 962-970.

[4] Librescu L, Marzocca P, Silva W A. Post-flutter instability of a shell type structures in hypersonic flow field. J Spacecraft and Rockets 2002; 39(5): 802-812.

[5] Librescu L, Chiocchia G, Marzocca P. Implications of cubic physical / aerodynamic nonlinearities on the character of the flutter instability boundary. Int J Nonlinear Mechanics 2003; 38(3): 173-199.

[6] Librescu L, Na S, Marzocca P, et al. Active aeroelastic control of 2-D wing-flap systems in an incompressible flow field. AIAA Paper 2003-1414, 2003.

[7] Qin Z, Marzocca P, Librescu L. Aeroelastic instability and response of advanced aircraft wings at subsonic flight speeds. J Aerospace Science and Technology 2002; 6(3): 195-208.

[8] Dowell E H. A modern course in aeroelasticity. Sijthoff and Noordhoff, Rockville, MD, 1978.

[9] Dowell E H, Edwards J, Strganac T. Nonlinear aeroelasticity J Aircraft 2003; 40(5): 857-874.

[10] Hyun D H, Lee I. Transonic and low-supersonic aeroelastic analysis of a two-degree-of-freedom airfoil with a freeplay nonlinearity. J of Sound and Vibration 2000; 234(5): 859-880.

[11] Block J, Heather Gilliatt. Active control of an aeroelastic structure. AIAA Paper-97-0016, 1997.

[12] Tang D M, Dowell E H, Virgil L N. Limit cycle behavior of an airfoil with a control surface. J Fluids and Structures 1998; 12(7): 839-858.

[13] Dario H B, Richard C L, Martin B. Robust aeroelastic matchpoint solutions using describing function method. J Aircraft 2005; 42(6): 1597-1605.

[14] Irving Abel. Research and applications in structures at the NASA Langley Research Center. NASA Technical Memorandum 110311, 1997.

[15] Michael W K, Lawrence C F. Aircraft ground vibration testing at the NASA Dryden Flight Research Facility–1993. NASA Technical Memorandum 104275, 1994.

[16] Mukhopadhyay V. Historical perspective on analysis and control of aeroelastic responses. J Guidance, Control, and Dynamics 2003; 26: 673-684.

[17] Horikawa H, Dowell E H. An elementary explanation of the flutter mechanism with active feedback controls. J Aircraft 1979; 16(4): 225-232.

[18] Vipperman J S, Dowell E H, Clark R L, et al. Investigation of the experimental active control of a typical section airfoil using trailing edge flap. J Aircraft 1998; 35: 224-229.

[19] Mukhopadhyay V. Benchmark active control technology. J Guidance, Control, and Dynamics 2000; Part I 23: 913-960, 2000, Part II 23: 1093-1139, 2001, Part III 24: 146-192.

[20] Na S, Librescu L, Marzocca P, et al. Robust aeroelastic control of flapped wing systems using a sliding mode observer. J Aerospace Science and Technology 2006; 10(2): 120-126.

[21] Lee B H K, Price S J, Wong Y S. Nonlinear aeroelastic analysis of airfoils: Bifurcation and chaos. Progress in Aerospace Sciences 1999; 35(3): 205-334.

[22] Hopf E. Bifurcation of a periodic solution from a stationary solution of a system of differential equations. Berlin Mathematische Physics Klasse, Sachsischen Akademic der Wissenschaften Leipzig 1942; 94: 3-32.

[23] Holmes P J. Bifurcations to divergence and flutter in flow-induced oscillations: A finite-dimensional analysis. J Sound and Vibration 1977; 53(4): 471-503.

[24] Mastroddi F, Morino L. Limit-cycle taming by nonlinear control with application to flutter. Aeronautical J 1996; 100(999): 389-396.

[25] Bisplinghoff R L, Ashley H. Principles of aeroelasticity. Dover, New York, 1996: 217-234.

[26] Zhao Y H, Hu H Y. Aeroelastic analysis of a nonlinear airfoil based on unsteady vortex lattice model. J Sound and Vibration 2004; 276(3-5): 491-510.

[27] Budiansky B, Mayers J. Influence of aerodynamic heating on the effective torsional stiffness of thin wings. J Aeronautical Sciences 1956; 23(12): 1081-1093, 1108.

[28] Lighthill M J. Oscillating airfoils at high Mach numbers. J Aeronautical Science 1953; 20(6): 402-406.

[29] Ashley H, Zartarian G. Piston theory – a new aerodynamic tool for the aeroelastician. J Aerospace Sciences 1956; 23(10): 1109- 1118.

[30] Thuruthimattam B B, Friedmann P P, McNamara J J, et al. Modeling approaches to hypersonic aeroelasticity. ASME Paper 2002-32943, 2002.

[31] Chavez F R, Liu D D. Unsteady unified hypersonic/supersonic method for aeroelastic applications including wave/shock Interaction. AIAA J 1995; 33(6): 1090-1097.

[32] Librescu L, Marzocca P, Silva W A. Supersonic/hypersonic flutter and post-flutter of geometrically imperfect circular cylindrical panels. J Spacecraft and Rockets 2002; 39(5): 802-812.

[33] Carafoli E, Berbente C. Determination of pressure and aerody-

namic characteristics of delta wings in supersonic–moderate hypersonic flow. Revue Roumaine des Sciences Techniques. Serie de Mecanique Appliquee 1966; 11(3): 587-613.

[34] Carafoli E, Mateescu D, Nastase A. Wing theory in supersonic flow. In: Jones R T, Jones W P, editors. International Series on Monographs in Aeronautics and Astronautics, Division 2: Aerodynamics, 7, Pergamon, Oxford, 1969: 463-524. (in Russian).

[35] Thuruthimattam B B, Friedmann P P, McNamara J J, et al. Aeroelasticity of a generic hypersonic vehicle. AIAA Paper 2002-1209, 2002.

[36] Laith K Abbas, Chen Q, Marzocca P, et al. Numerical studies of a nonlinear aeroelastic system with plunging and pitching freeplays in supersonic/hypersonic regimes. Aerospace Science and Technology J 2007; 11(5): 405-418.

Biography:

Laith K Abbas Born in 1965, he received B.S., M.S. and Ph.D. from former M.E.C., Baghdad, Iraq in 1987, 1995 and 2002 respectively, and then became a teacher at the Technical Education Department, University of Technology. Now he is a postdoctoral research fellow for two years since October 2005 in Institute of Vibration Engineering Research, College of Aerospace Engineering, Nanjing University of Aeronautics and Astronautics.

E-mail: laith.detec@nuaa.edu.cn, laithabbass@yahoo.com